



HAL
open science

Pasireotide and octreotide antiproliferative effects and sst2 trafficking in human pancreatic neuroendocrine tumor cultures.

Amira Mohamed, Marie-Pierre Blanchard, Manuela Albertelli, Federica Barbieri, Thierry Brue, Patricia Niccoli, Jean-Robert Delpero, Genevieve Monges, Stephane Garcia, Diego Ferone, et al.

► To cite this version:

Amira Mohamed, Marie-Pierre Blanchard, Manuela Albertelli, Federica Barbieri, Thierry Brue, et al.. Pasireotide and octreotide antiproliferative effects and sst2 trafficking in human pancreatic neuroendocrine tumor cultures.. *Endocrine-Related Cancer*, 2014, 21 (5), pp.691-704. 10.1530/ERC-14-0086 . hal-01176951

HAL Id: hal-01176951

<https://hal.science/hal-01176951v1>

Submitted on 23 Apr 2018

HAL is a multi-disciplinary open access archive for the deposit and dissemination of scientific research documents, whether they are published or not. The documents may come from teaching and research institutions in France or abroad, or from public or private research centers.

L'archive ouverte pluridisciplinaire **HAL**, est destinée au dépôt et à la diffusion de documents scientifiques de niveau recherche, publiés ou non, émanant des établissements d'enseignement et de recherche français ou étrangers, des laboratoires publics ou privés.

Pasireotide and octreotide antiproliferative effects and sst₂ trafficking in human pancreatic neuroendocrine tumor cultures

Amira Mohamed^{1,2}, Marie-Pierre Blanchard³, Manuela Albertelli⁴, Federica Barbieri⁴, Thierry Brue^{1,5}, Patricia Niccoli⁶, Jean-Robert Delpero⁷, Genevieve Monges⁸, Stephane Garcia⁹, Diego Ferone⁴, Tullio Florio⁴, Alain Enjalbert^{1,2}, Vincent Moutardier¹⁰, Agnes Schonbrunn¹¹, Corinne Gerard¹, Anne Barlier^{1,2,*} and Alexandru Saveanu^{1,2,*}

¹Aix-Marseille Université, CNRS, CRN2M-UMR 7286, Faculté de Médecine, Secteur Nord – CS80011, 51, Bd Pierre Dramard, 13344 Marseille Cedex 15, France

²Molecular Biology Laboratory, AP-HM, Conception Hospital, 13385 Marseille, France

³Aix-Marseille Université, CNRS, Plate-Forme de Recherche en Neurosciences PFRN, 13344 Marseille Cedex 15, France

⁴Department of Internal Medicine and Center of Excellence for Biomedical Research, University of Genova, Genova, Italy

⁵Endocrinology Department, AP-HM, Timone Hospital, 13385 Marseille, France

⁶Oncology Department, ⁷Surgery Department, and ⁸Biopathology Department, Paoli Calmettes Cancer Institute, 13009 Marseille, France

⁹Pathology Laboratory, and ¹⁰Surgery Department, AP-HM, Nord Hospital, 13015 Marseille, France

¹¹Department of Integrative Biology and Pharmacology, University of Texas, Texas 77225, Houston, USA

* (A Saveanu and A Barlier contributed equally to this work)

Correspondence should be addressed to A Saveanu or A Barlier
Email
alexandru.saveanu@univ-amu.fr or
anne.barlier@univ-amu.fr

Abstract

Gastroenteropancreatic neuroendocrine tumors (GEP–NETs) raise difficult therapeutic problems despite the emergence of targeted therapies. Somatostatin analogs (SSA) remain pivotal therapeutic drugs. However, the tachyphylaxis and the limited antitumoral effects observed with the classical somatostatin 2 (sst₂) agonists (octreotide and lanreotide) led to the development of new SSA, such as the pan sst receptor agonist pasireotide. Our aim was to compare the effects of pasireotide and octreotide on cell survival, chromogranin A (CgA) secretion, and sst₂ phosphorylation/trafficking in pancreatic NET (pNET) primary cells from 15 tumors. We established and characterized the primary cultures of human pancreatic tumors (pNETs) as powerful preclinical models for understanding the biological effects of SSA. At clinically relevant concentrations (1–10 nM), pasireotide was at least as efficient as octreotide in inhibiting CgA secretion and cell viability through caspase-dependent apoptosis during short treatments, irrespective of the expression levels of the different sst receptors or the WHO grade of the parental tumor. Interestingly, unlike octreotide, which induces a rapid and persistent partial internalization of sst₂ associated with its phosphorylation on Ser341/343, pasireotide did not phosphorylate sst₂ and induced a

Key Words

- ▶ octreotide
- ▶ pasireotide
- ▶ human pancreatic neuroendocrine tumors
- ▶ receptor trafficking
- ▶ somatostatin receptors
- ▶ primary culture

rapid and transient internalization of the receptor followed by a persistent recycling at the cell surface. These results provide the first evidence, to our knowledge, of striking differences in the dynamics of sst₂ trafficking in pNET cells treated with the two SSAs, but with similar efficiency in the control of CgA secretion and cell viability.

Endocrine-Related Cancer
(2014) 21, 691–704

Introduction

Gastroenteropancreatic neuroendocrine tumors (GEP-NETs) constitute a rare group of tumors, with a significant increase in incidence and prevalence in the past few decades (Oberge 2011). GEP-NETs still raise difficult therapeutic problems despite the emergence of targeted therapies such as rapalogs (inhibitors of the mammalian target of rapamycin; Yao *et al.* 2011) or tyrosine kinase inhibitors (Raymond *et al.* 2011). Despite numerous clinical trials testing various strategies, progression-free survival or overall survival remain limited. In this context, it would be of interest to develop relevant preclinical models.

Among all pharmacological tools, the somatostatin analogs (SSA), octreotide and lanreotide, remain the pivotal therapeutic molecules for controlling hormone-related symptoms of functioning GEP-NETs (Rubin *et al.* 1999, O'Toole *et al.* 2000, Modlin *et al.* 2010). However, the initial antisecretory potency of SSA decreases with long-term treatment. The mechanisms potentially involved in this adaptation (or tachyphylaxis) to continuous exposure to SSA are not yet clearly understood (Hofland & Lamberts 2003). These drugs also have antitumor activity, as demonstrated in the PROMID and CLARINET studies (Rinke *et al.* 2009, Caplin *et al.* 2014). However, less than 5% of patients have objective radiological tumor regression (Rinke *et al.* 2009). Moreover, 50% of patients display stabilization of tumor size, but this antitumoral effect concerns NET classified as a 'good prognosis' (Baudin *et al.* 2012).

GEP-NETs express multiple somatostatin (sst) receptors: sst₂ (in 70–100% of tumors; Reubi *et al.* 2001, Papotti *et al.* 2002, O'Toole *et al.* 2006), but also sst₁ and/or sst₅ and/or sst₃. The two commercial SSA, octreotide and lanreotide, are octapeptides that bind with high affinity to sst₂ and with moderate affinity to sst₅. The failures of these classical SSA have led to the development of new SSA such as pasireotide. This molecule i) binds avidly to sst₅ and sst₂ and more mildly to sst₃ and sst₁ (Schmid & Silva 2005), ii) is able to suppress adrenocorticotrophic hormone secretion in Cushing's disease, mainly through sst₅ (Boscaro *et al.* 2009), and iii) induces differential sst₂

trafficking, as shown in the heterologous model HEK 293 cells (Pöll *et al.* 2010) as well as in rat pancreatic Ar42J tumor cells (Kao *et al.* 2011). Together, these data raise the question of its use in GEP-NETs. In a phase II clinical trial, pasireotide has been shown to control symptoms related to carcinoid syndrome in 27% of patients with NETs who were resistant to octreotide (Kvols *et al.* 2012). However, the effects of pasireotide in comparison to octreotide on tumor secretion and proliferation and its relationship to WHO grades, sst expression profile, and sst trafficking in GEP-NETs remain to be explored.

For somatotroph adenomas, our group previously demonstrated that sensitivities to SSA are strongly correlated *in vivo* (in patient) and *in vitro* (in culture of tumor primary cells from the same patient) (Jaquet *et al.* 2000). Under these conditions, the use of human tumoral cells in primary culture might be a relevant strategy for evaluating the therapeutic effect of different drugs, particularly of SSA.

In this study, we established and characterized, for the first time, to our knowledge, primary cell cultures of human pancreatic NETs (pNETs). We show that pNET primary cells in culture retained neuroendocrine characteristics such as expression and secretion of chromogranin A (CgA), expression of the different subtypes of sst receptors, and sensitivity to octreotide at concentrations used *in vivo*. We then used this model to evaluate the effects of pasireotide on cell viability, CgA secretion, and on sst₂ phosphorylation and trafficking in comparison with octreotide.

Patients and methods

Patients

This study was approved by the Ethics Committee of the Aix-Marseille University (Aix-Marseille, France) and informed consent was obtained from each patient. Fifteen patients with GEP-NET tumors were included in the study (Table 1). Patients underwent surgery. Fourteen tumors were located in the pancreas (pNETs); one was a hepatic metastasis of a pNET. In 13 cases, there was no clinical or biochemical evidence of hormonal hypersecretion, thus

Table 1 Clinical and immunohistochemical characteristics of 15 human pNETs

Tumor (number)	Age (years)	Sex	Tumor (mm)	Ki67 (%)	Grade
T1	53	F	15	<2	G1
T2	59	M	35 ^b	3	G2
T3	67	M	25	90	G3
T4	27	F	17	1	G1
T5	69	M	55 ^b	<1	G1
T6	65	M	12	4	G2
T7	64	M	26 ^a	1	G1
T8	49	F	45 ^b	13	G2
T9	66	F	50	6	G2
T10	58	F	70 ^c	<2	G1
T11	53	F	15	5	G2
T12	45	M	27	10	G2
T13	26	F	37 ^a	1.2	G1
T14	36	F	49 ^a	5	G2
T15	67	F	44	3	G2

Tumor size is expressed as maximal diameter (mm). For primary tumors associated with (a) multiple localization, (b) positive lymph node, (c) hepatic metastasis and positive lymph node, tumor size is the sum of the diameters for each localization. Grade is determined according to WHO classification.

they were considered as nonfunctional pNETs. In two cases, the tumors were secreting and symptomatic: insulinoma (T4) and gastrinoma (T10), confirmed by pathology report. Determination of Ki67 and proliferation index allowed grade classification (WHO 2010 classification; Table 1).

Pharmacological compounds

The SSAs, octreotide and pasireotide, were provided by Novartis AG. Forskolin and isobutylmethylxanthine (IBMX) were from Sigma–Aldrich and calyculin A from Ozyme (St Quentin les Yvelines, France).

Cell culture

Tumor fragments of human pNETs, obtained after surgery, were dissociated mechanically and enzymatically (Jaquet *et al.* 1985). The tumoral cells were seeded on 24-, 12-, or four-well plates (according to the experiments) coated with extracellular matrix (ECM) (from bovine endothelial corneal cells as previously described (Jaquet *et al.* 1985)) required for cell adhesion. The cells were maintained in a culture in L-valine-depleted DMEM (L-valine was replaced by D-valine to block fibroblast proliferation), supplemented with 10% FCS, penicillin (100 U/ml), streptomycin (100 µg/ml), and glutamine (100 U/ml) at

37 °C in a water-saturated atmosphere containing 7% CO₂. Determination of the sst mRNA levels, cell viability, and CgA secretion was carried out on cell cultures of all the tumors. Other experiments were performed according to the quantity of tumoral cells available after dissociation of each tumor. All the experiments were done in D-valine DMEM containing 5% FCS.

Real-time quantitative PCR

Total mRNAs were extracted from 3 × 10⁵ cells using the RNeasy Microkit (Qiagen). The receptor mRNAs, sst₁, sst₂, sst₃, and sst₅, were detected by real-time quantitative PCR using specific primers and probes as described previously (Saveanu *et al.* 2001). To produce standard curves, cDNA constructs were produced for each variable, verified by sequencing (Beckman Coulter Ceq 8000 (Beckman Coulter, Fullerton, CA, USA)), and linearized. The mRNA levels of each receptor subtype were normalized to the glucuronidase β (*GUSB*) mRNA level, as described previously (Saveanu *et al.* 2001). The results were expressed as copy of mRNA for the sst gene/copy of mRNA for *GUSB*.

Cell viability

The cells from each tumor were seeded into 24-well plates (4 × 10⁴ cells/well). After 24 h in culture, the cells were treated without or with octreotide or pasireotide at the indicated concentrations for 72 h. The medium was recovered for CgA determination, and cell viability was assayed by a luminescent cell viability assay (CellTiter Glo; Promega) according to the manufacturer's protocol. Results were expressed as percentages of the value for the control cells (in the absence of the analogs).

CgA secretion

CgA secretion was determined on the medium recovered from cell viability experiments after 72 h of treatment in the presence or absence of the analogs (see above). The recovered culture media were centrifuged at 400 g and stored at –20 °C. CgA was measured using a commercial ELISA Kit (Chromogranin A ELISA Kit, Dako, Les Ulis, France) according to the manufacturer's protocol. Basal tumoral secretion of the cells from each tumor in culture was reported as U/l CgA per 72 h (Table 2). The effects of drugs on CgA secretion were expressed as percentages of the value for the control group.

Table 2 Chromogranin A secretion and sst mRNA expression in primary cultures from 15 human pNETs

Tumor (number)	CgA secretion		mRNA expression (copies/copy <i>GUSB</i>)			
	Control (U/l)	Octreotide (% inhibition)	sst ₁	sst ₂	sst ₃	sst ₅
T1	170 ± 5	51 ± 3 [‡]	0.34	4.94	0.09	0.04
T2	49 ± 0	76 ± 5 [‡]	0.13	0.96	0.03	–
T3	10 ± 1	60 ± 3 [‡]	0.04	0.32	–	0.06
T4	76 ± 1	75 ± 2 [‡]	0.40	0.16	0.05	0.02
T5	16 ± 2	55 ± 1*	4.21	3.23	0.69	0.15
T6	870 ± 125	73 ± 1 [‡]	0.28	0.88	0.05	0.18
T7	735 ± 33	69 ± 2 [‡]	1.55	2.35	0.86	0.30
T8	21 ± 2	47 ± 1 [†]	0.01	0.54	–	–
T9	93 ± 19	86 ± 3 [†]	0.40	3.65	–	0.04
T10	568 ± 21	63 ± 10 [†]	0.78	2.67	–	0.67
T11	569 ± 48	33 ± 1*	0.77	2.75	0.41	0.05
T12	488 ± 10	88 ± 2 [†]	3.51	0.5	0.02	–
T13	115 ± 7	84 ± 1 [‡]	3.53	5.45	1.80	0.42
T14	691 ± 87	81 ± 4 [‡]	0.63	0.96	0.01	–
T15	325 ± 9	29 ± 0 [†]	0.74	2.80	0.65	–

The cells were cultured without or with 10 nM octreotide for 72 h and CgA was determined as described in the 'Patients and methods' section. sst receptor mRNAs were determined as described in the 'Patients and methods' section by real-time PCR. –, undetectable. **P* < 0.05, [†]*P* < 0.01, and [‡]*P* < 0.001.

Apoptosis measurement

DNA fragmentation measurement The cells from each tumor were seeded on 14 mm ECM-coated coverslips in four-well tissue culture plates (10⁵ cells/well). After 24 h in culture, cells were treated without or with octreotide or pasireotide (1 nM) for 24 h. The cells were fixed with 1% paraformaldehyde in PBS for 15 min at room temperature. DNA fragmentation was detected by TUNEL with the Apoptotag Red *In Situ* Apoptosis Detection Kit (Millipore, Molsheim, France), according to the manufacturer's protocol. The apoptotic cells were then viewed with a Leica/Leitz DMRB microscope using a PL fluotar ×100 objective and scored manually. Results were expressed as the number of TUNEL-positive cells/total cells in 40 successive fields per condition for each cell culture.

Determination of caspase activity The cells from each tumor were seeded into 24-well plates (4 × 10⁴ cells/well). After 24 h in culture, the cells were treated without or with octreotide or pasireotide (1 nM) for 24 h. The activity of the executioner caspases 3 and 7 was measured using the Caspase Glo 3/7 Assay (Promega) according to the manufacturer's protocol. Results were expressed as a percentage of the value for the control conditions.

cAMP assay

The cells from each tumor were seeded into 24-well plates (4 × 10⁴ cells/well). After 24 h in culture, the cAMP

concentration was determined using the HTRF-cAMP Femto Kit (CisBio International, Bagnols-sur-Cèze, France), as described previously (Cuny *et al.* 2012). According to the manufacturer's protocol, the cells were detached using trypsin, seeded onto 96-well plates in suspension, and incubated at 37 °C for 3 h in the presence of 1 μM forskolin and 0.1 μM IBMX (control condition) or combined with 1 nM octreotide or pasireotide. The HTRF assay reagents were then added directly into the 96-well plates. The results were expressed as a percentage of the value for the control conditions.

Immunocytochemistry

The cells from each tumor were seeded on 14 mm ECM-coated coverslips in four-well tissue culture plates (10⁵ cells/well). After 24 h in culture, the cells were treated without or with 1 nM octreotide or pasireotide for the times indicated. The cells were fixed with 4% paraformaldehyde in PBS for 10 min at room temperature and incubated overnight at 4 °C with the primary antibodies: rabbit antisera against sst₂ (SS-800; Gramsch Lab, Schwabhausen, Germany, 1:1000), rabbit antisera against the Ser341/343-phosphorylated sst₂ receptor antibody (Ra-1124, 1:1000) (Ghosh & Schonbrunn 2011), or rabbit antisera against CgA (Novus biological Europe, Cambridge, UK, 1:200). To detect phosphorylated sst₂, the cells were preincubated for 30 min with 100 nM calyculin A (serine/threonine phosphatase inhibitor, Ozyme, St Quentin en Yvelines, France). The Alexa Fluor 488-conjugated goat anti-rabbit IgG (Molecular

Probes, Life Technologies, Saint Aubin, France, 1:800 in PBS containing 10% non-immune goat serum) was used as secondary antibody. The coverslips were mounted in 'ProlongGold' including DAPI for nuclei staining (Life Technologies).

Confocal images were acquired on a Zeiss LSM780 laser-scanning microscope equipped with a $63\times$ (1, 4 n.a.) oil immersion lens with a zoom factor of 1 or 4. The images of sst-Alexa 488 and DAPI-stained cells were respectively obtained using the 488-nm band of an Argon laser and 405 nm diode. Spectral detection of emitted fluorescence was set as follows: 495–535 nm for Alexa 488 and 410–475 nm for DAPI. Images were collected automatically as frame-by-frame z-series. The pinhole was adjusted to the first Airy disk. The pictures presented are single optical slices. Immunocytochemistry experiments were performed on primary cultures from nine pNETs (T2, T3, T4, T6, T7, T10, T13, T14, and T15).

Image analysis and quantification of the sst₂ receptor

Gray-level confocal images (8-bit) of sst₂ staining were analyzed and quantified using ImageJ Software (<http://imagej.nih.gov/ij/list.html>). For each cell, mean gray values were measured along a five pixel-width line drawn at the cell periphery, considered to be membrane immunostaining. For cytoplasmic staining, gray values of three distinct regions covering most of cytoplasm were determined. Mean gray values were measured on four successive optical slices. Twelve cells were selected at random from each cell culture for each experimental condition. The results were expressed as the ratio of peripheral sst₂ immunostaining to total immunostaining as a percentage of the control value.

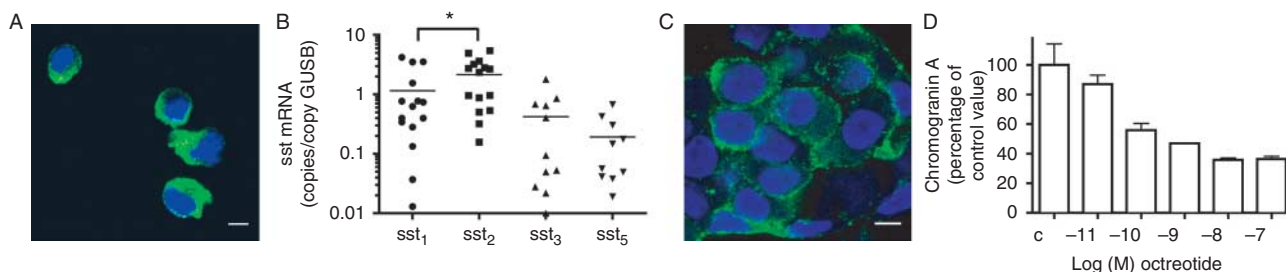


Figure 1

Characterization of pNET primary cells in culture. (A) Immunostaining of chromogranin A (CgA) as described in the 'Patients and methods' section in a representative pNET primary culture (T13) ($63\times$, zoom factor 1). Nuclei are stained in blue (DAPI), CgA is shown in green. Scale bar: 10 μm . (B) sst₁, sst₂, sst₃, and sst₅ mRNA levels in primary cultures from 15 human pNETs were determined by real-time PCR. Results were normalized to the level of *GUSB* mRNA and are reported as copies/copy *GUSB*. The horizontal bars represent the means.

Statistical analysis

Each assay was performed in triplicate. Results are presented as the mean \pm s.e.m. of triplicate determinations of a representative tumor (Fig. 1D) or mean \pm s.e.m. of at least three tumors. The statistical significance between two paired groups was determined by the Wilcoxon's non-parametric test and those between two unpaired groups by the Mann-Whitney *U* nonparametric test. To measure the strength of association between pairs of variables without specifying dependency, Spearman's rank order correlations were run. The differences were considered statistically significant at $P \leq 0.05$.

Results

Establishment and characterization of pNET primary cells in culture

Fifteen pNETs were successfully dissociated to obtain primary cells in culture. Under our culture conditions, cells from all tumors secreted CgA in a range of 10–870 U/l per 72 h (Table 2). As illustrated in Fig. 1A (T13), positive CgA immunolabeling was observed in all cells, showing that they were neuroendocrine cells.

The sst₂ and sst₁ mRNAs were expressed in the cells from all tumors. The sst₂ expression level was higher than the sst₁ level in 80% of tumors (mean mRNA levels, 2.07 ± 0.44 and 1.15 ± 0.36 copy/copy *GUSB* respectively, Fig. 1B and Table 2). sst₃ and sst₅ mRNAs were expressed in 73 and 67% of cases respectively (Table 2). The expression levels of the sst receptors did not differ significantly with respect to the WHO grade of the tumor, except for sst₅, which was expressed in 100% of grade 1 tumors and only in 37% of

* $P < 0.03$. (C) Immunostaining of sst₂ receptor in a representative pNET primary culture (T2) ($63\times$, zoom factor 1). Nuclei are stained in blue (DAPI); sst₂ is shown in green. Scale bar: 10 μm . (D) Cells were incubated without (c) and with octreotide at the indicated concentrations for 72 h and CgA was determined as described in the 'Patients and methods' section. Results from one representative pNET (T6) are expressed as mean \pm s.e.m. of triplicate determinations as percentages of the value for the controls (in the absence of octreotide).

grade 2 tumors (Tables 1 and 2). Despite differences in the quantitative levels of the sst receptors due to the presence of other sst-expressing cell types in the tissue, sst expression profiles were similar to those of the primary tumor tissues (data not shown).

Given that sst₂ is the main target of SSA and is not expressed in fibroblasts, expression of the sst₂ protein was analyzed by immunocytochemistry in cells from eight pNET tumors (T2, T3, T4, T6, T7, T10, T14, T13, none of which had been pretreated with SSA before surgery). Immunoreactivity of sst₂ was found in almost 100% of cells in all of the tumors investigated, as illustrated in Fig. 1C (T2). In the absence of SSA, sst₂ immunoreactivity was mainly located on the plasma membrane and to a lesser extent in the cytoplasm (Fig. 1C). This confirmed that, under our culture conditions, an overwhelming majority of cells were neuroendocrine cells, and that fibroblast proliferation was contained.

Finally, the functionality of sst₂ was explored by testing the effect of octreotide on CgA secretion. As illustrated in Fig. 1D (T6), octreotide displayed a dose-dependent inhibition of CgA secretion. An octreotide-dependent decrease in CgA secretion was significantly observed in all investigated tumors in a range of 29–88% for 10 nM octreotide (Table 2). There was no correlation between maximal inhibition of CgA secretion and the sst expression levels or the WHO grade of the tumor.

Effect of pasireotide and octreotide on cell viability

The effects of octreotide and pasireotide on cell viability were determined for the characterized pNET primary cultures. Both analogs reduced viable cell number in the primary cultures from all 15 tumors (Fig. 2A). Maximal inhibition, observed at 1 or 10 nM for each drug, ranged from 23 to 86% with octreotide and from 16 to 79% with pasireotide

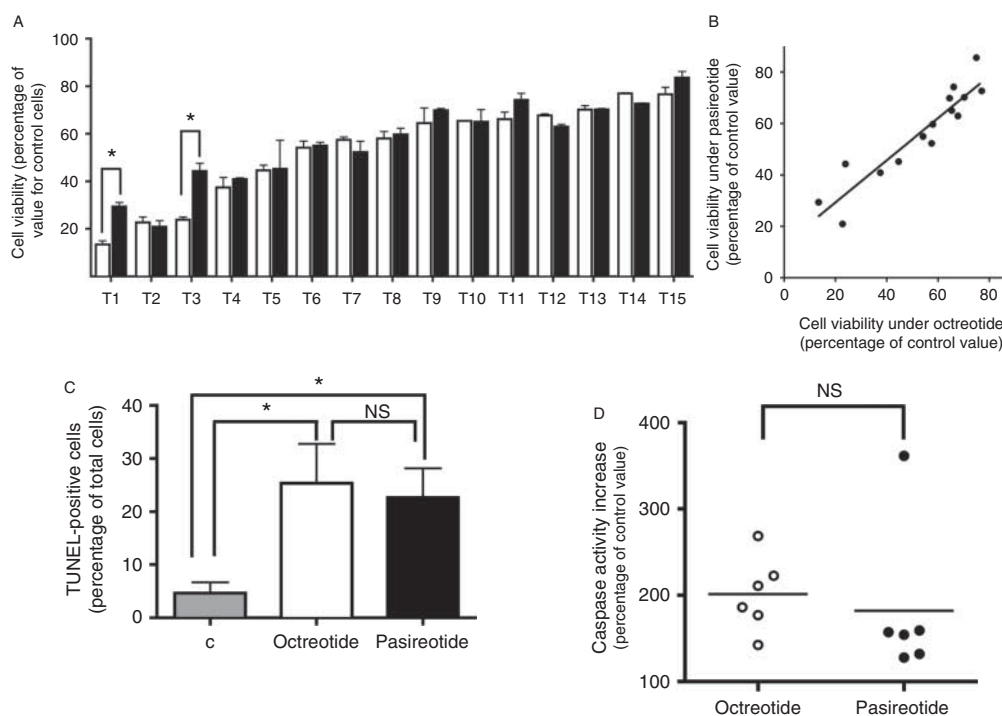


Figure 2

Pasireotide and octreotide similarly decrease cell viability through caspase-dependent apoptosis. (A) Primary culture cells from 15 pNETs were incubated without and with 1–10 nM octreotide (white bars) or 1–10 nM pasireotide (black bars) for 72 h and cell viability was determined as described in the 'Patients and methods' section. Results are expressed as mean \pm s.e.m. of triplicate determinations as percentages of the control value. Maximal inhibition is given. * $P < 0.01$. (B) Correlation between maximal inhibition of cell viability induced by octreotide and pasireotide in the same tumor ($R = 0.92$, $P < 0.0001$). (C) Primary culture cells from three pNETs (T9, T11, and T13) were incubated without (gray bar) and with 1 nM

octreotide (white bar) or 1 nM pasireotide (black bar) for 24 h and DNA fragmentation was determined by TUNEL assay as described in the 'Patients and methods' section. Results are expressed as the mean of triplicate determinations for each primary cell culture as percentages of the control value. The horizontal bars represent the means. NS, not significant.

(Fig. 2A). A significant difference between the effects of octreotide and pasireotide on maximal cell viability inhibition was observed in only two cases: T1 and T3 (Fig. 2A). A strong correlation was observed between the effects of both analogs (Fig. 2B). There was no correlation between the maximal inhibition of cell viability with octreotide or pasireotide and the mRNA levels of the different subtypes of ssts. Moreover, pasireotide did not induce better inhibition in tumor cells expressing high levels of sst_1 , sst_5 , or sst_3 .

For two patients, one bearing tumor T2 and the other T13, it was possible to analyze the effect of analogs on two tumoral sites, the primary tumor and a metastatic lymph node for the T2 patient, and two different pancreatic tumors for the T13 patient. In both cases, there were no significant differences in cell viability inhibition for the two tumoral sites, either with octreotide or pasireotide (data not shown).

To determine the mechanism underlying the reduction in the number of viable cells induced by octreotide and pasireotide, DNA fragmentation was investigated using a TUNEL assay on primary cultures from three tumors (T9, T11, and T13). Both octreotide and pasireotide increased the number of apoptotic events (Fig. 2C), indicating an apoptotic mechanism. The apoptotic effect of octreotide and pasireotide was further investigated by measuring the activity of the executioner caspases. Basal caspase activity in untreated cells was significantly increased by octreotide and pasireotide in all the primary cultures from six tumors (201.3 ± 17.7 and $182.1 \pm 36.3\%$, respectively, $P < 0.03$; Fig. 2D; T1, T3, T7, T8, T13, and T15). So both analogs induced caspase-dependent apoptotic cell death in pNET primary cells.

Effect of pasireotide and octreotide on CgA secretion

The antisecretory effect of pasireotide was then determined and compared with that of octreotide. Pasireotide dose-dependently decreased CgA secretion, similarly to octreotide, in the primary cultures from all the tumors (Fig. 3A). Although the decrease in cell number observed under SSA treatment, as described above, potentially has an effect on CgA secretion, inhibition of CgA secretion by octreotide and pasireotide was still observed after 'normalization' of CgA secretion data against cell viability. Under these conditions, CgA secretion represents 36 ± 7 and $41 \pm 5\%$ ($n = 15$) of the value for controls for 1 nM SSA treatment respectively, indicating direct effects of SSA on CgA secretion mechanisms. A good correlation was observed between maximal inhibitions of CgA secretion under

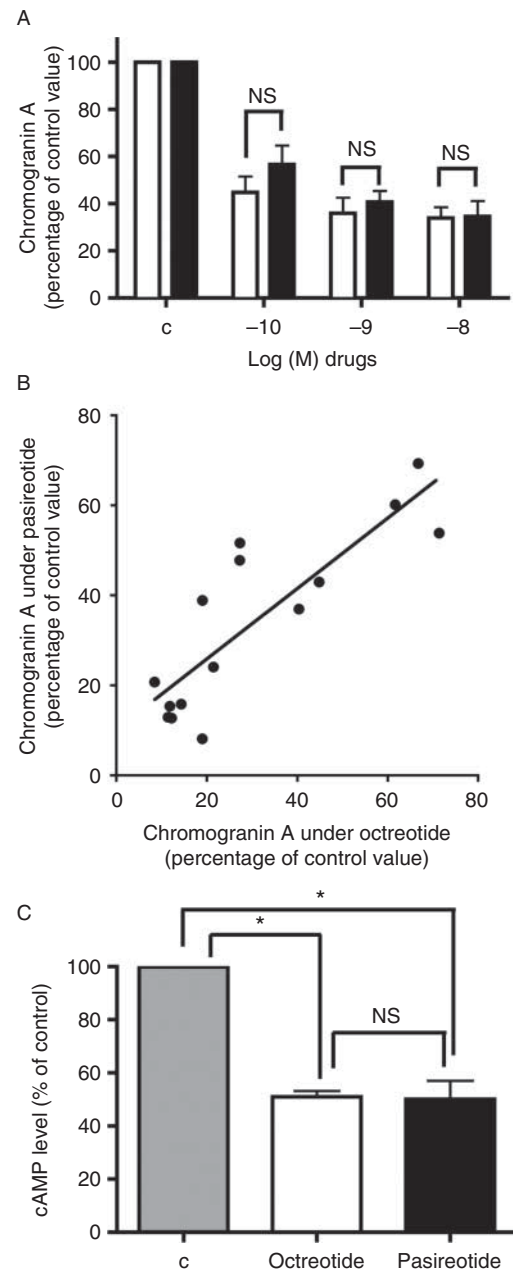


Figure 3

Pasireotide and octreotide similarly decrease CgA secretion and cAMP levels. (A) Primary culture cells from 15 pNETs were incubated without (c) levels and with the indicated concentration of octreotide (white bars) or pasireotide (black bars) for 72 h and CgA was measured as described in the 'Patients and methods' section. Results are expressed as mean \pm s.e.m. ($n = 15$) as a percentage of the value for controls. Each assay was performed in triplicate. (B) Correlation between maximal CgA inhibition induced by octreotide and pasireotide in the same tumor ($R = 0.82$, $P < 0.0001$). (C) Primary culture cells from three pNETs (T5, T9, and T10) were incubated in the presence of 1 μ M forskolin and 0.1 μ M IBMX and without (gray bar) or with 1 nM octreotide (white bar) or 1 nM pasireotide (black bar), and then cAMP levels were determined as described in the 'Patients and methods' section. Results are expressed as mean \pm s.e.m. ($n = 3$) as a percentage of the value for the controls. Each assay was performed in triplicate. * $P < 0.01$; NS, not significant.

pasireotide and octreotide (Fig. 3B). No correlation was observed between maximal inhibitions of CgA and the mRNA levels of the different subtypes of sst. Moreover, there was no correlation between the inhibitions observed on cell viability and on CgA secretion for each analog (not shown).

Given that cAMP is one of the main molecules involved in the inhibition of hormonal secretion induced by SSA (Hofland & Lamberts 2003), the effect of octreotide and pasireotide on the intracellular cAMP levels was investigated using primary cultures from three tumors (T5, T9, and T10). Octreotide and pasireotide similarly reduced the

cAMP level (by 49 ± 2 and $50 \pm 6\%$, respectively, Fig. 3C), in agreement with the similar antisecretory effect observed for the two analogs on the pNET primary cells.

Time course of sst₂ internalization and recycling under pasireotide and octreotide

The time course of sst₂ trafficking under pasireotide and octreotide treatment was then investigated by sst₂ immunolabeling in pNET primary cells. In primary cultures from seven tumors (T2, T3, T6, T7, T10, T14, and T13), sst₂ internalization was rapidly observed after 5 min of

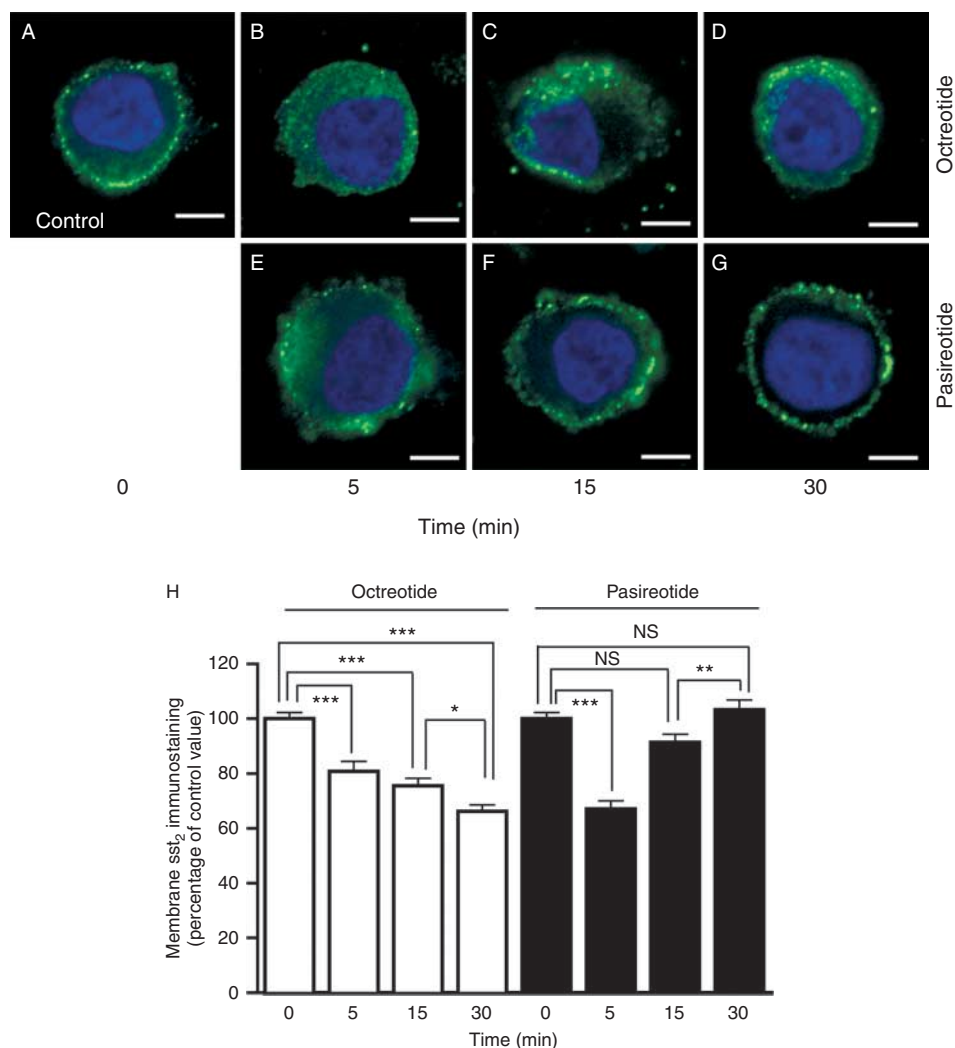


Figure 4

Differential time course of sst₂ internalization with pasireotide and octreotide. Primary cells in culture (T2) were incubated without (A) and with 1 nM octreotide (B, C and D) or 1 nM pasireotide (E, F and G) for the time indicated. sst₂ is shown in green and nuclei are stained in blue (DAPI), zoom factor 4, Scale bars: 5 μm. (H) Quantification of membrane sst₂ immunostaining in T2 and T14, as described in the 'Patients and methods'

section, in the presence of octreotide (white bars) or pasireotide (black bars) for the time indicated. Results are expressed as mean \pm s.e.m. as a percentage of the level of control immunostaining in each experimental condition. * $P < 0.05$; ** $P < 0.01$; *** $P < 0.001$; NS, not significant. Membrane sst₂ immunostaining under control conditions is $71 \pm 3\%$ of total sst₂ immunostaining.

octreotide treatment, as illustrated in Fig. 4B (T2), and was maintained in the cytosol up to 30 min (Fig. 4C and D; T2). The quantification of sst_2 's subcellular localization showed that sst_2 labeling at the cell surface progressively decreased and reached $66 \pm 2\%$ of control sst_2 immunostaining level after 30 min exposure to octreotide (Fig. 4H; T2 and T14).

Five minutes of pasireotide treatment also induced sst_2 internalization, as illustrated in Fig. 4E (T2). In contrast, after 15 min of pasireotide treatment, sst_2 immunolabeling was mainly observed at the cell surface (Fig. 4F and G; T2). The quantification of sst_2 's subcellular localization in the presence of pasireotide showed that sst_2 labeling at the cell surface represented $67 \pm 3\%$ of the control level of sst_2 immunostaining after 5 min of pasireotide exposure and progressively recovered to the control level (Fig. 4H; T2 and T14), indicating membrane recycling of the receptor.

To investigate whether the differential sst_2 localization observed under octreotide/pasireotide persisted after long-term exposure, immunocytochemical analysis of sst_2 was carried out after 1 and 24 h SSA treatment. After 1 and 24 h of treatment with pasireotide, the sst_2 receptor was mainly located at the cell surface (Fig. 5F and G; T10). In contrast, with octreotide treatment, sst_2 distribution was similar to that observed at 5–30 min, still mainly in the cytosol (Fig. 5C and D; T10).

Time course of sst_2 phosphorylation with pasireotide and octreotide

Finally, sst_2 phosphorylation, which is strongly involved in receptor trafficking, was investigated in pNET primary cells, using an antibody specific for the sst_2 receptor phosphorylated at Ser341/343 (psst₂). In untreated cells, no psst₂ immunostaining was detected (Fig. 6A; T15) whereas sst_2 receptor immunostaining was present at the cell surface (Fig. 6B; T15). After 5 and 30 min exposure to 1 nM octreotide, clusters of psst₂ were detected, both at the cell surface and in the cytosol (Fig. 6C and D; T15). In contrast, no phosphorylation of the sst_2 receptor was detected after 5 and 30 min exposure to 1 nM pasireotide (Fig. 6E and F; T15).

Discussion

For the first time, we have established and characterized primary cell cultures of human GEP-NETs. Tumoral cells of pNETs have a slow growth rate *in vitro* and low adhesion to plastic or the available commercial matrix (A Mohamed, 2011 unpublished observations). Using bovine ECM, we obtained monolayers of neuroendocrine cells that retain CgA expression and secretion, expression of the different subtypes of sst receptors, and sst_2

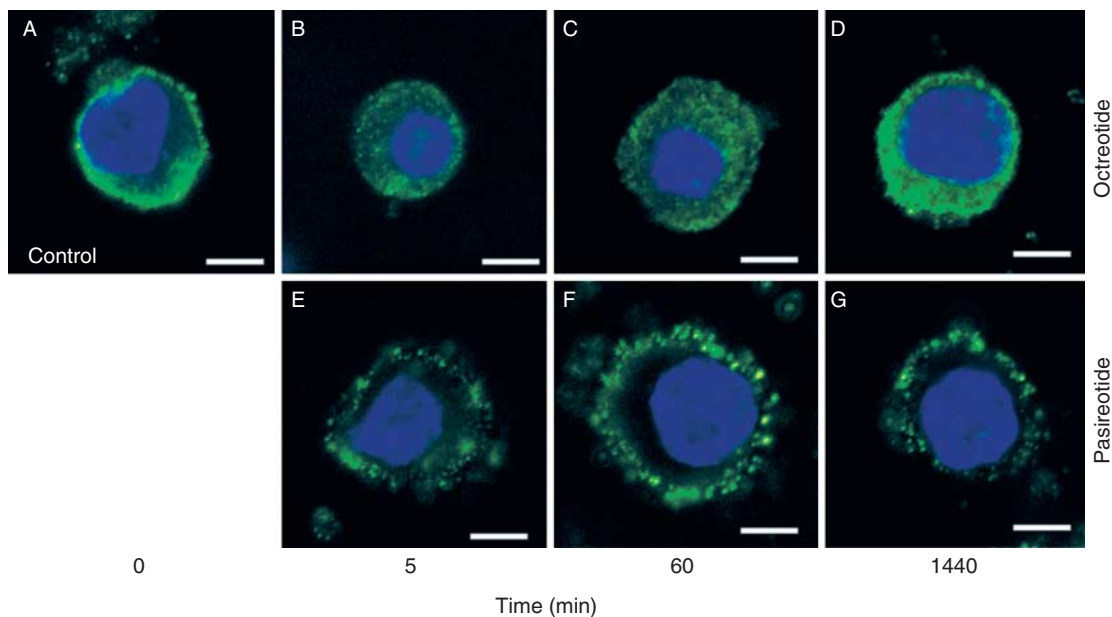
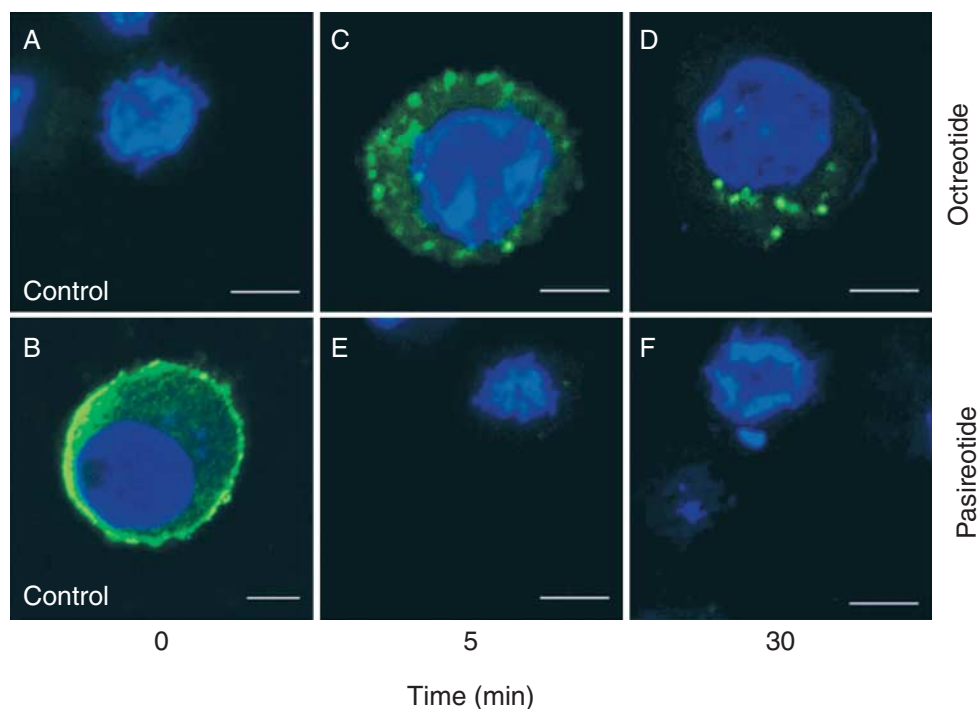


Figure 5

Pasireotide and octreotide induce differential localization of sst_2 during long-term exposure. Primary cells in culture were incubated without (A) and with 1 nM octreotide (B, C and D) or 1 nM pasireotide (E, F and G) for

the time indicated. sst_2 is shown in green and nuclei are stained in blue (DAPI), zoom factor 4. Scale bars: 5 μ M. Results from one representative tumor (T10) are shown.

**Figure 6**

Pasireotide and octreotide induce differential phosphorylation of sst_2 on Ser341/343. Primary cells in culture were incubated without (A and B) and with 1 nM octreotide (C and D) or 1 nM pasireotide (E and F) for the times indicated.

sst_2 is shown in green (B), sst_2 phosphorylation on Ser341/343 is shown in green (A, C, D, E and F), and nuclei are stained in blue (DAPI), zoom factor 4. Scale bars: 10 μ M. Results from one representative tumor (T15) are shown.

functionality. The sst expression patterns in the primary cells of pNETs were similar to those previously found in GEP-NET tumor tissues by our group (O'Toole *et al.* 2006) and by others (Reubi *et al.* 2001, Papotti *et al.* 2002, Ono *et al.* 2007, Srirajskanthan *et al.* 2009, Kim *et al.* 2011): sst_2 remains the primary sst expressed, sst_1 is the secondary subtype expressed, both in terms of percentage of positive tumors and of quantitative mRNA level.

In the human pNET BON1 cell line, which expresses sst_2 , the antiproliferative effect of octreotide is not clearly observed *in vitro* (BON cells in culture) or *in vivo* (BON cell xenografts) (Moreno *et al.* 2008). Concentrations of octreotide above 1 μ M are required to produce small amounts of growth inhibition (Georgieva *et al.* 2010). In contrast, in the pNET primary cultures described herein, the concentrations of octreotide (1 nM) needed to decrease cell viability and CgA secretion were similar to those found in the plasma of treated patients (Woltering *et al.* 2008). So the drawbacks of cell lines, even of human origin, for testing pharmacological molecules may be resolved by the use of pNET primary cells in culture.

In all the primary cultures from the 15 human pNETs studied, pasireotide decreased cell viability and

CgA secretion. Pasireotide has a 40-, 30-, and fivefold higher binding affinity than octreotide for sst_5 , sst_1 , and sst_3 , respectively and a 2.5-fold lower affinity for sst_2 (Schmid 2008). In pNET cells, despite the expression of sst_1 , sst_3 , and sst_5 , pasireotide was not more efficient than octreotide. Similar inhibitory effects on cell viability and CgA secretion were observed for pasireotide and octreotide at concentrations found in the plasma of treated patients (from 1 to 10 nM for octreotide (Woltering *et al.* 2008) and about 8 nM for pasireotide (Kvols *et al.* 2012)). Note that pasireotide induces growth inhibition with an IC₅₀ 1000-fold superior in the BON1 cell line (Somnay *et al.* 2013). In our study, both analogs decreased cell viability by caspase-dependent apoptosis and repressed cAMP levels, which could be involved in the inhibition of CgA secretion. The inhibitory effect of SSA on CgA secretion even after 'normalization' of CgA secretion against cell number and lack of correlation between SSA effects on cell viability and on CgA secretion indicate that the mechanisms underlying antitumor effects and control of secretion by SSA are independent. Moreover strong correlations were observed between the effects of both analogs on cell viability as well as on CgA secretion. All together, these results strongly

indicate that under our experimental conditions, pasireotide acts mainly through ss_{t_2} (which is the most expressed receptor) in pNET primary cells in culture. To our knowledge, no comparison has been made of the effects of pasireotide and octreotide in GEP-NET patients naïve to SSA treatments.

We used pNET cells in culture to explore the dynamics of ss_{t_2} trafficking and phosphorylation under octreotide and pasireotide treatment. In untreated cells, ss_{t_2} was not phosphorylated and was mainly located at the cell surface. A clinically relevant concentration of octreotide (1 nM) induced a rapid and persistent partial ss_{t_2} internalization associated with its phosphorylation on Ser341/343. These results are consistent with observations showing that excised GEP-NET tumors of untreated patients display exclusively nonphosphorylated expression of ss_{t_2} on the cell surface, whereas tumors of octreotide-treated patients contain Ser341/343 phosphorylated ss_{t_2} , predominantly internalized (Reubi *et al.* 2010, Waser *et al.* 2012). In the same way, we show for the first time, to our knowledge, in pNET cells in culture, striking differences in ss_{t_2} trafficking under a clinically relevant concentration of pasireotide (1 nM). Pasireotide induced a rapid and transient internalization of ss_{t_2} followed by a persistent re-expression of the receptor at the cell surface. Surprisingly Ser341/343 phosphorylation was not observed under pasireotide even at 5 min. This could be explained by massive and rapid recycling of the receptor, which requires its dephosphorylation during internalization before reinsertion into the plasma membrane. The lack of Ser phosphorylation (critical for ss_{t_2} desensitization/uncoupling; Liu *et al.* 2008, Kao *et al.* 2011) indicates that the level of active receptors at the cell surface is greater with chronic pasireotide than with octreotide.

The differential patterns of ss_{t_2} internalization induced by pasireotide and octreotide have been shown in the HEK 293 cell line transfected either with human ss_{t_2} (hs ss_{t_2} ; Lesche *et al.* 2009) or with rat ss_{t_2} (rs ss_{t_2} ; Pöll *et al.* 2010). In the study of Lesche and colleagues, pasireotide was less potent than octreotide in inducing hs ss_{t_2} internalization and required 30 min exposure to 1 μ M pasireotide. In the study of Pöll and colleagues, rs ss_{t_2} internalization is not observed after 5-min exposure to 10 μ M pasireotide. Moreover, in contrast to octreotide, a lack of ss_{t_2} internalization with pasireotide has also been observed in the rat pituitary and pancreas *in vivo* after 90-min exposure (Pöll *et al.* 2010). A close correlation between the phosphorylation levels of a cluster of four threonine residues, within the cytoplasmic C-terminal region of ss_{t_2} , and ss_{t_2} internalization has been established under pasireotide and octreotide treatments in

rs ss_{t_2} -transfected HEK 293 cells: octreotide but not pasireotide is able to increase threonine phosphorylation and induces ss_{t_2} internalization (Pöll *et al.* 2010). It has similarly been shown that pasireotide is less effective than sst (ss14) in inducing endogenous ss_{t_2} internalization in pancreatic Ar42J cells or in rs ss_{t_2} receptor-transfected CHOK1, and this lesser internalization is associated with less phosphorylation of both Ser341/343 and Thr353/354 (Kao *et al.* 2011). In addition, in that study, arrestins were less recruited to the membrane and formed more unstable complexes with ss_{t_2} under pasireotide than under ss14. Moreover ss_{t_2} was more rapidly dephosphorylated and recycled after pasireotide treatment than ss14 treatment (Kao *et al.* 2011). It has also been shown that GRK2 is required for ss14-stimulated ss_{t_2} phosphorylation on Ser341/343 (Liu *et al.* 2009) and that GRK2/GRK3 are required for ss14-dependent phosphorylation of ss_{t_2} on Thr353/354 (Pöll *et al.* 2010). Furthermore, overexpression of GRK2 increases pasireotide-dependent phosphorylation and internalization of ss_{t_2} (Pöll *et al.* 2010). Recently, GRK2 and β -arrestin 1 mRNA levels were found to be correlated with octreotide response in human GH adenomas (Gatto *et al.* 2013). Therefore besides the determination of the sst expression profiles, assessment of GRK and arrestin levels would be of interest for predicting the extent of ss_{t_2} internalization/recycling and biological effects with SSA therapy.

Taken together, our results on primary cultures of pNET cells provide strong evidence for the existence of differential patterns of ss_{t_2} phosphorylation and internalization/recycling with clinically relevant concentrations of octreotide and pasireotide, as previously demonstrated in ss_{t_2} -transfected heterologous cell lines and in a rat pancreatic tumor cell line endogenously expressing the ss_{t_2} receptor (recently reviewed by Reubi & Schonbrunn (2013)).

The differential ss_{t_2} trafficking in pNET primary cells during treatment with pasireotide and octreotide observed in this study, does not initiate different biological effects. Although ss_{t_2} internalization/desensitization is greater in the presence of octreotide, the decreased number of active receptors at the cell surface might be compensated for by the different affinity of octreotide for ss_{t_2} and for the other sst receptors, relative to the affinity of pasireotide. Moreover, independently of the differential ss_{t_2} trafficking, both analogs could recruit the same downstream signaling cascades. These might account for the similar biological effects we observed for the two analogs over the timescale studied.

Octreotide can control hormonal-related symptoms in patients initially. However, some responsive tumors escape after prolonged treatment and become resistant

to octreotide (Modlin *et al.* 2010). Although clinical observations of tachyphylaxis in GEP-NET during octreotide treatment are well established, the underlying mechanisms are still elusive. Preliminary results of the phase III study conducted to compare pasireotide LAR with octreotide LAR in patients inadequately controlled by conventional doses of SSA indicate that long-term GEP-NET treatment with pasireotide LAR may be of benefit (Clinical Trial number NTC00690430, unpublished results (Wolin *et al.* 2013)). Under these conditions, it would be of interest to explore the localization and the phosphorylation status of ss_{t_2} in tumors of pasireotide-treated patients, as has been previously performed for octreotide (Reubi *et al.* 2010, Waser *et al.* 2012), to confirm or rebut our observations on pasireotide-persistent membrane expression of ss_{t_2} under continuous treatment.

Escape from response to octreotide observed over months or years is unlikely to be due to rapid uncoupling or internalization of the receptor (Hofland & Lamberts 2003, Reubi & Schonbrunn 2013). It is rather more likely that it could be due to changes in the expression or recruitment of crucial signaling partners downstream of the ss_{t_2} receptor or change in proteins that regulate receptor function (Reubi & Schonbrunn 2013). Recently, Li *et al.* (2012) have shown that 16 months of continuous exposure to octreotide still decreased cell growth of CNDT.2.5 (a small intestine NET-derived cell line) and progressively upregulated several genes involved in growth/differentiation and cell signaling. Therefore, tachyphylaxis might be associated with the downregulation of such genes. How the dynamics of the receptor, encoded by chronic agonist binding, could be involved in such processes requires further investigations.

In conclusion, the experiments described in this study are the first investigation, to our knowledge, of the role of pasireotide and octreotide in primary culture of human pNET cells. It is shown that at clinically relevant concentrations, pasireotide is at least as efficient as octreotide for repressing hormonal secretion and cell viability despite the striking difference in ss_{t_2} trafficking between pasireotide and octreotide treatment in pNET cells. Finally, pNET cells in primary cultures could be considered as a relevant preclinical model i) to improve our understanding of ss_{t_2} receptor pharmacology and ii) to study biological effects in development of new drugs.

Declaration of interest

The authors declare that there is no conflict of interest that could be perceived as prejudicing the impartiality of the research reported.

Funding

This work was supported by Centre National pour la Recherche Scientifique (UMR 7286), Aix-Marseille Université, Association pour le Développement des Recherches Biologiques et Médicales au Centre Hospitalier Régional de Marseille (A.D.E.R.E.M.), Protisvalor Méditerranée (Aix-Marseille Université), and Novartis Pharma SAS. A Mohamed was a recipient of a fellowship from the A.D.E.R.E.M. (2010/2011). This study was partially supported by Novartis Pharma SAS.

Author contribution statement

The authors have made the following declarations about their contributions: A Mohamed: set-up of GEP-NETs primary cultures, pharmacological studies, chromogranin A, cell viability assessment, and immunocytochemistry studies; M-P Blanchard: immunocytochemistry studies by confocal microscopy; M Albertelli and F Barbieri: set-up of primary culture of GEP-NETs; T Brue, P Niccoli, and J-R Delpero: correlation between clinical data and *in vitro* functional data, scientific discussions; G Monges and S Garcia: immunohistochemical analysis of the tumor and WHO grade determination; D Ferone and T Florio: set-up of primary culture of GEP-NETs, establishment of the project and scientific discussions; V Moutardier: correlation between clinical data and *in vitro* functional data and scientific discussions; A Enjalbert: data analysis and scientific discussions; A Schonbrunn: set-up of $psst_2$ antibody experiments and scientific discussions; C Gerard: data analysis, scientific discussions, and drafting of the paper; A Barlier: scientific direction of the project, data analysis, and drafting of the paper; and A Saveanu: scientific direction of the project, real-time PCR of ss_{t_2} , data analysis, scientific discussions, and drafting of the paper.

Acknowledgements

The authors thank Anne Laure Germanetti for technical advice on qRT-PCR studies and Gary Burkhart for his help with correcting the English.

References

- Baudin E, Planchard D, Scoazec J-Y, Guigay J, Dromain C, Hadoux J, Debaere T, Elias D & Ducreux M 2012 Intervention in gastroenteropancreatic neuroendocrine tumours. *Best Practice & Research. Clinical Gastroenterology* **26** 855–865. (doi:10.1016/j.bpg.2013.01.008)
- Boscaro M, Ludlam WH, Atkinson B, Glusman JE, Petersenn S, Reincke M, Snyder P, Tabarin A, Biller BM, Findling J *et al.* 2009 Treatment of pituitary-dependent Cushing's disease with the multireceptor ligand somatostatin analog pasireotide (SOM230): a multicenter, phase II trial. *Journal of Clinical Endocrinology and Metabolism* **94** 115–122. (doi:10.1210/jc.2008-1008)
- Caplin ME, Pavel M, Cwikla JB, Phan AT, Raderer M, Sedláčková E, Cadiot G, Wolin EM, Capdevila J, Wall L *et al.* 2014 Lanreotide in metastatic enteropancreatic neuroendocrine tumors. *New England Journal of Medicine* **371** 224–233. (doi:10.1056/NEJMoa1316158)
- Cuny T, Mohamed A, Graillon T, Roche C, Defilles C, Germanetti A-L, Couderc B, Figarella-Branger D, Enjalbert A, Barlier A *et al.* 2012 Somatostatin receptor ss_{t_2} gene transfer in human prolactinomas *in vitro*: impact on sensitivity to dopamine, somatostatin and dopastatin, in the control of prolactin secretion. *Molecular and Cellular Endocrinology* **355** 106–113. (doi:10.1016/j.mce.2012.01.026)
- Gatto F, Feelders R, van der Pas R, Kros JM, Dogan F, van Koetsveld PM, van der Lelij A-J, Neggers SJ, Minuto F, de Herder W *et al.* 2013 β -Arrestin 1 and 2 and G protein-coupled receptor kinase 2 expression in pituitary adenomas: role in the regulation of response to

- somatostatin analogue treatment in patients with acromegaly. *Endocrinology* **154** 4715–4725. (doi:10.1210/en.2013-1672)
- Georgieva I, Koychev D, Wang Y, Holstein J, Hopfenmüller W, Zeitz M & Grabowski P 2010 Zm447439, a novel promising aurora kinase inhibitor, provokes antiproliferative and proapoptotic effects alone and in combination with bio- and chemotherapeutic agents in gastroenteropancreatic neuroendocrine tumor cell lines. *Neuroendocrinology* **91** 121–130. (doi:10.1159/000258705)
- Ghosh M & Schonbrunn A 2011 Differential temporal and spatial regulation of somatostatin receptor phosphorylation and dephosphorylation. *Journal of Biological Chemistry* **286** 13561–13573. (doi:10.1074/jbc.M110.215723)
- Hofland LJ & Lamberts SW 2003 The pathophysiological consequences of somatostatin receptor internalization and resistance. *Endocrine Reviews* **24** 28–47. (doi:10.1210/er.2000-0001)
- Jaquet P, Gunz G & Grisoli F 1985 Hormonal regulation of prolactin release by human prolactinoma cells cultured in serum-free conditions. *Hormone Research* **22** 153–163. (doi:10.1159/000180089)
- Jaquet P, Saveanu A, Gunz G, Fina F, Zamora AJ, Grino M, Culler MD, Moreau JP, Enjalbert A & Ouafik LH 2000 Human somatostatin receptor subtypes in acromegaly: distinct patterns of messenger ribonucleic acid expression and hormone suppression identify different tumoral phenotypes. *Journal of Clinical Endocrinology and Metabolism* **85** 781–792. (doi:10.1210/jcem.85.2.6338)
- Kao YJ, Ghosh M & Schonbrunn A 2011 Ligand-dependent mechanisms of sst2A receptor trafficking: role of site-specific phosphorylation and receptor activation in the actions of biased somatostatin agonists. *Molecular Endocrinology* **25** 1040–1054. (doi:10.1210/me.2010-0398)
- Kim HS, Lee HS & Kim WH 2011 Clinical significance of protein expression of cyclooxygenase-2 and somatostatin receptors in gastroenteropancreatic neuroendocrine tumors. *Cancer Research and Treatment* **43** 181–188. (doi:10.4143/crt.2011.43.3.181)
- Kvols LK, Oberg KE, O'Dorisio TM, Mohideen P, de Herder WW, Arnold R, Hu K, Zhang Y, Hughes G, Anthony L et al. 2012 Pasireotide (SOM230) shows efficacy and tolerability in the treatment of patients with advanced neuroendocrine tumors refractory or resistant to octreotide LAR: results from a phase II study. *Endocrine-Related Cancer* **19** 657–666. (doi:10.1530/ERC-11-0367)
- Lesche S, Lehmann D, Nagel F, Schmid H & Schulz S 2009 Differential effects of octreotide and pasireotide on somatostatin receptor internalization and trafficking in vitro. *Journal of Clinical Endocrinology and Metabolism* **94** 654–661. (doi:10.1210/jc.2008-1919)
- Li S-C, Martijn C, Cui T, Essaghir A, Luque RM, Demoulin J-B, Castaño JP, Öberg K & Giandomenico V 2012 The somatostatin analogue octreotide inhibits growth of small intestine neuroendocrine tumour cells. *PLoS ONE* **7** e48411. (doi:10.1371/journal.pone.0048411)
- Liu Q, Dewi DA, Liu W, Bee MS & Schonbrunn A 2008 Distinct phosphorylation sites in the sst2A somatostatin receptor control internalization, desensitization, and arrestin binding. *Molecular Pharmacology* **73** 292–304. (doi:10.1124/mol.107.038570)
- Liu Q, Bee MS & Schonbrunn A 2009 Site specificity of agonist and second messenger-activated kinases for somatostatin receptor subtype 2A (sst2A) phosphorylation. *Molecular Pharmacology* **76** 68–80. (doi:10.1124/mol.108.054262)
- Modlin IM, Pavel M, Kidd M & Gustafsson BI 2010 Review article: somatostatin analogues in the treatment of gastroenteropancreatic neuroendocrine (carcinoid) tumours. *Alimentary Pharmacology & Therapeutics* **31** 169–188. (doi:10.1111/j.1365-2036.2009.04174.x)
- Moreno A, Akcakanat A, Munsell MF, Soni A, Yao JC & Meric-Bernstam F 2008 Antitumor activity of rapamycin and octreotide as single agents or in combination in neuroendocrine tumors. *Endocrine-Related Cancer* **15** 257–266. (doi:10.1677/ERC-07-0202)
- O'Toole D, Ducreux M, Bommelaer G, Wemeau JL, Bouché O, Catus F, Blumberg J & Ruszniewski P 2000 Treatment of carcinoid syndrome: a prospective crossover evaluation of lanreotide versus octreotide in terms of efficacy, patient acceptability, and tolerance. *Cancer* **88** 770–776. (doi:10.1002/(SICI)1097-0142(20000215)88:4<770::AID-CNCR6>3.0.CO;2-0)
- O'Toole D, Saveanu A, Couvelard A, Gunz G, Enjalbert A, Jaquet P, Ruszniewski P & Barlier A 2006 The analysis of quantitative expression of somatostatin and dopamine receptors in gastro-entero-pancreatic tumours opens new therapeutic strategies. *European Journal of Endocrinology* **155** 849–857. (doi:10.1530/eje.1.02307)
- Oberg K 2011 Neuroendocrine tumors: recent progress in diagnosis and treatment. *Endocrine-Related Cancer* **18** (Suppl 1) E3–E6. (doi:10.1530/ERC-10-0288)
- Ono K, Suzuki T, Miki Y, Taniyama Y, Nakamura Y, Noda Y, Watanabe M & Sasano H 2007 Somatostatin receptor subtypes in human non-functioning neuroendocrine tumors and effects of somatostatin analogue SOM230 on cell proliferation in cell line NCI-H727. *Anticancer Research* **27** 2231–2239.
- Papotti M, Bongiovanni M, Volante M, Allia E, Landolfi S, Helboe L, Schindler M, Cole SL & Bussolati G 2002 Expression of somatostatin receptor types 1–5 in 81 cases of gastrointestinal and pancreatic endocrine tumors. a correlative immunohistochemical and reverse-transcriptase polymerase chain reaction analysis. *Virchows Archiv* **440** 461–475. (doi:10.1007/s00428-002-0609-x)
- Pöll F, Lehmann D, Illing S, Ginj M, Jacobs S, Lupp A, Stumm R & Schulz S 2010 Pasireotide and octreotide stimulate distinct patterns of sst_{2A} somatostatin receptor phosphorylation. *Molecular Endocrinology* **24** 436–446. (doi:10.1210/me.2009-0315)
- Raymond E, Dahan L, Raoul J-L, Bang Y-J, Borbath I, Lombard-Bohas C, Valle J, Metrakos P, Smith D, Vinik A et al. 2011 Sunitinib malate for the treatment of pancreatic neuroendocrine tumors. *New England Journal of Medicine* **364** 501–513. (doi:10.1056/NEJMoa1003825)
- Reubi JC & Schonbrunn A 2013 Illuminating somatostatin analog action at neuroendocrine tumor receptors. *Trends in Pharmacological Sciences* **34** 676–688. (doi:10.1016/j.tips.2013.10.001)
- Reubi J, Schaer J-C & Laussie J 2001 Somatostatin receptor sst1–sst5 expression in normal and neoplastic human tissues using receptor autoradiography with subtype-selective ligands. *European Journal of Nuclear Medicine and Molecular Imaging* **28** 836–846. (doi:10.1007/s002590100541)
- Reubi JC, Waser B, Cescato R, Gloor B, Stettler C & Christ E 2010 Internalized somatostatin receptor subtype 2 in neuroendocrine tumors of octreotide-treated patients. *Journal of Clinical Endocrinology and Metabolism* **95** 2343–2350. (doi:10.1210/jc.2009-2487)
- Rinke A, Müller H-H, Schade-Brittinger C, Klose K-J, Barth P, Wied M, Mayer C, Aminossadati B, Pape U-F, Bläker M et al. 2009 Placebo-controlled, double-blind, prospective, randomized study on the effect of octreotide LAR in the control of tumor growth in patients with metastatic neuroendocrine midgut tumors: a report from the PROMID Study Group. *Journal of Clinical Oncology* **27** 4656–4663. (doi:10.1200/JCO.2009.22.8510)
- Rubin J, Ajani J, Schirmer W, Venook AP, Bukowski R, Pommier R, Saltz L, Dandona P & Anthony L 1999 Octreotide acetate long-acting formulation versus open-label subcutaneous octreotide acetate in malignant carcinoid syndrome. *Journal of Clinical Oncology* **17** 600–606.
- Saveanu A, Gunz G, Dufour H, Caron P, Fina F, Ouafik L, Culler MD, Moreau JP, Enjalbert A & Jaquet P 2001 BIM-23244, a somatostatin receptor subtype 2- and 5-selective analog with enhanced efficacy in suppressing growth hormone (GH) from octreotide-resistant human GH-secreting adenomas. *Journal of Clinical Endocrinology and Metabolism* **86** 140–145. (doi:10.1210/jcem.86.1.7099)
- Schmid HA 2008 Pasireotide (SOM230): development, mechanism of action and potential applications. *Molecular and Cellular Endocrinology* **286** 69–74. (doi:10.1016/j.mce.2007.09.006)
- Schmid HA & Silva AP 2005 Short- and long-term effects of octreotide and SOM230 on GH, IGF-I, ACTH, corticosterone and ghrelin in rats. *Journal of Endocrinological Investigation* **28** (11 Supplement International) 28–35.

- Somnay Y, Chen H & Kunnimalaiyaan M 2013 Synergistic effect of pasireotide and terflunomide in carcinoids *in vitro*. *Neuroendocrinology* **97** 183–192. (doi:10.1159/000341810)
- Srirajaskanthan R, Watkins J, Marelli L, Khan K & Caplin ME 2009 Expression of somatostatin and dopamine 2 receptors in neuroendocrine tumours and the potential role for new biotherapies. *Neuroendocrinology* **89** 308–314. (doi:10.1159/000179899)
- Waser B, Cescato R, Liu Q, Kao YJ, Körner M, Christ E, Schonbrunn A & Reubi JC 2012 Phosphorylation of sst2 receptors in neuroendocrine tumors after octreotide treatment of patients. *American Journal of Pathology* **180** 1942–1949. (doi:10.1016/j.ajpath.2012.01.041)
- Wolin EM, Jarzab B, Eriksson B, Walter T, Toumpanakis C, Morse M, Tomassetti P, Weber M, Fogelman D, Ramage J et al. 2013 A multicenter, randomized, blinded, phase III study of pasireotide LAR versus octreotide LAR in patients with metastatic neuroendocrine tumors (NET) with disease-related symptoms inadequately controlled by somatostatin analogs. *International Journal of Clinical Oncology* **31** (suppl; abstr 4031). 2013 ASCO Annual Meeting.
- Woltering EA, Salvo VA, O'Dorisio TM, Lyons J, Li G, Zhou Y, Seward JR, Go VL, Vinik AI, Mamikunian P et al. 2008 Clinical value of monitoring plasma octreotide levels during chronic octreotide long-acting repeatable therapy in carcinoid patients. *Pancreas* **37** 94–100. (doi:10.1097/MPA.0b013e31816907ab)
- Yao JC, Shah MH, Ito T, Bohas CL, Wolin EM, Van Cutsem E, Hobday TJ, Okusaka T, Capdevila J, de Vries EG et al. 2011 Everolimus for advanced pancreatic neuroendocrine tumors. *New England Journal of Medicine* **364** 514–523. (doi:10.1056/NEJMoa1009290)

Received in final form 10 June 2014

Accepted 8 July 2014

Made available online as an Accepted Preprint

10 July 2014